Acta Cryst E CRYSTALLOGRAPHIC COMMUNICATIONS

ISSN 2056-9890

Synthesis, crystal structure and Hirshfeld surface analysis of bis(2-amino-1,3,4-thiadiazol-3-ium) diaquadichlorido(propanedioato-κ^2O^1,O^3)-manganate(II)

Guzal Nuralieva,[a] Mushtari Alieva,[a,b] Ekaterina Kinshakova,[a] Aziz Atashov,[c] Jamshid Ashurov,[d] Shakhnoza Kadirova[a] and Batirbay Torambetov[a]*

[a]National University of Uzbekistan named after Mirzo Ulugbek, 4 University St, Tashkent, 100174, Uzbekistan, [b]Tashkent Pharmaceutical Institute, 45 A. Aybek St. Tashkent, 100015, Uzbekistan, [c]Karakalpak State University, 1 Ch.Abdirov St. Nukus, 230112, Uzbekistan, and [d]Institute of Bioorganic Chemistry, Academy of Sciences of Uzbekistan, M. Ulugbek St, 83, Tashkent, 100125, Uzbekistan. *Correspondence e-mail: torambetov_b@mail.ru

Received 1 December 2025
Accepted 3 February 2026

Edited by M. Weil, Vienna University of Technology, Austria

Keywords: crystal structure; manganese(II) complex; malonato ligand; thiadiazolium cation; hydrogen bonding; supramolecular interactions.

CCDC reference: 2495418

Supporting information: this article has supporting information at journals.iucr.org/e

In the title salt, $(C_2H_4N_3S)_2[MnCl_2(C_3H_2O_4)(H_2O)_2]$, the central Mn^{II} atom of the complex anion adopts a distorted octahedral coordination environment, defined by two aqua, two chlorido, and one bidentate malonato ligands. The anion is charge balanced by two thiadiazole moieties protonated at one of the heterocyclic N atoms. In the crystal, the cations and anions engage in extensive hydrogen-bonding interactions and short S···Cl contacts; additional π–π stacking interactions are present between adjacent cations. Hirshfeld surface analysis was used to quantify the intermolecular interactions of the complex anion, revealing that H···O, H···Cl, and H···H interactions contribute most to the crystal packing.

1. Chemical context

The 1,3,4-thiadiazole ring is a five-membered aromatic heterocycle with different isomeric forms (1,2,3-thiadiazole, 1,2,4-thiadiazole, 1,2,5-thiadiazole, and 1,3,4-thiadiazole). The 1,3,4-isomer is the most extensively studied due to its wide range of biological and pharmacological activities, including antimicrobial, antifungal, antitubercular, anti-inflammatory, anticonvulsant, antioxidant, antihypertensive, and anticancer effects (Ahmad *et al.*, 2024; Parmar & Umrigar, 2017; Hu *et al.*, 2014; Kinshakova *et al.*, 2025; Chou *et al.*, 2003). Additionally, the N–C–S moiety within the 1,3,4-thiadiazole ring enables strong coordination with metal ions through its nitrogen and sulfur donor atoms, forming stable metal complexes (Lynch, 2002; Zhu *et al.*, 2017; Kadirova *et al.*, 2022; Atashov *et al.*, 2024). This combination of biological efficacy and coordination versatility underscores its importance in both medicinal and coordination chemistry. Several metal complexes are known to exhibit enhanced biological activities compared to the control or parent ligand/drug after complex formation (Femi & Ayoola, 2012). In particular, manganese complexes have been shown to possess promising biological activities; however, they remain relatively underexplored and insufficiently studied (Kozieł *et al.*, 2024).

In this article, we report on a salt consisting of cations from a 1,3,4-thiadiazole derivative and a manganese-based anion containing aqua, chlorido and malonato ligands, $(LH)_2[MnCl_2(C_3H_2O_4)(H_2O)_2]$ (L is 2-amino-1,3,4-thiadiazole, $C_2H_3N_3S$).

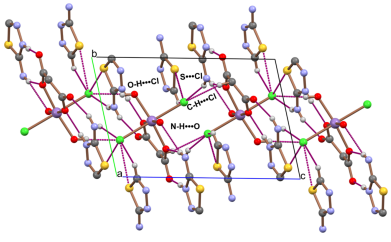

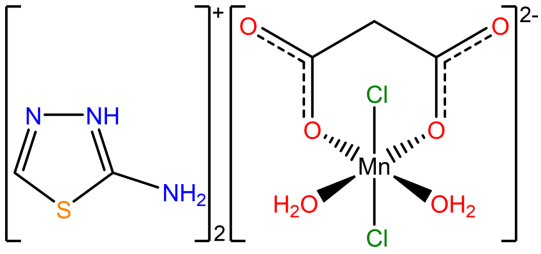

2. Structural commentary

The asymmetric unit of $(LH)_2[Mn(H_2O)_2Cl_2(C_3O_4H_2)]$ comprises two $(LH)^+$ cations, both protonated on the N atom at the 3-position of the heterocycle (atom numbering N1 and N4), and one $[Mn(H_2O)_2Cl_2(C_3O_4H_2)]^{2-}$ dianion (Fig. 1). The central manganese(II) atom is distorted octahedrally coordinated by two aqua ligands, two chlorido ligands, and one malonato ligand, which acts as a bidentate ligand through two of its carboxylate oxygen atoms. The two chlorido ligands are situated *trans* to each other at the axial positions, while the equatorial plane is defined by the bidentate malonato ligand and the two *cis*-positioned aqua ligands. The Mn—O bond lengths range from 2.136 (3) to 2.194 (3) Å, while the Mn—Cl bonds are significantly longer [2.5363 (14) to 2.6243 (13) Å]. From the coordination environment and charge balance, the oxidation state of the manganese ion is determined to be +II.

3. Supramolecular features

$(LH)_2[Mn(H_2O)_2Cl_2(C_3O_4H_2)]$ exhibits an intricate network of intermolecular interactions due to the presence of multiple hydrogen-bonding sites. These include N—H···O, N—H···Cl, and C—H···Cl interactions with the donor sites located at the two thiadiazolium cations, and with O—H···O, O—H···N and O—H···Cl interactions of the aqua ligands. Numerical details are given in Table 1. In addition, short S···Cl contacts between the cations and anion are present, ranging from 3.1867 (18) to 3.4457 (17) Å, shorter than the sum of the van der Waals radii for S and Cl (≈3.55 Å; Bondi, 1964), as well as a π–π stacking interaction between two adjacent thiadiazolium cations, with a centroid-to-centroid distance of 3.620 (3) Å (slippage: 1.338 Å, *Cg*2···*g*3(–1 + *x*, −1 + *y*, *z*); *Cg*2 and *Cg*3 are the centroids of the S1–C4–N1–N2–C5 and S2–C6–N4–N5–C7 rings, respectively). The packing of the molecules is shown in Fig. 2.

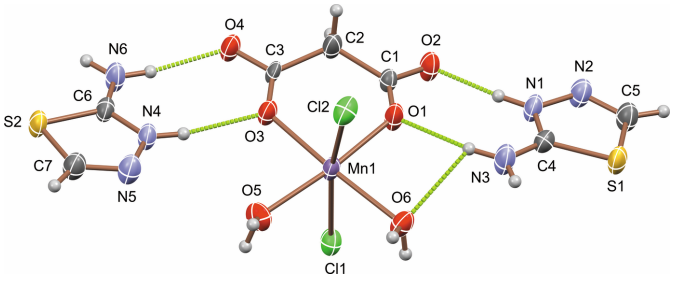

Figure 1
The asymmetric unit of $(LH)_2[Mn(H_2O)_2Cl_2(C_3O_4H_2)]$ drawn with displacement ellipsoids at the 50% probability level; hydrogen atoms are displayed as small spheres of arbitrary size. Intermolecular hydrogen-bonding interactions are shown as green dashed lines.

Table 1
Hydrogen-bond geometry (Å, °).

D—H···*A*	*D*—H	H···*A*	*D*···*A*	*D*—H···*A*
O5—H5*A*···O2^{i}	0.85 (1)	1.93 (2)	2.761 (5)	166 (5)
O5—H5*B*···Cl1^{ii}	0.85 (1)	2.34 (1)	3.186 (4)	175 (7)
O6—H6*A*···O4^{iii}	0.85	2.08	2.853 (5)	151
O6—H6*B*···N2^{i}	0.85	2.06	2.866 (5)	158
N1—H1···O2	0.86	1.78	2.641 (5)	175
N3—H3*A*···O1	0.86	2.02	2.854 (5)	162
N3—H3*B*···Cl2^{iv}	0.86	2.39	3.207 (5)	158
N4—H4···O3	0.86	2.07	2.919 (5)	171
N6—H6*C*···O4	0.86	1.92	2.760 (5)	165
N6—H6*D*···Cl1^{v}	0.86	2.45	3.243 (4)	154
N6—H6*D*···Cl1^{vi}	0.86	2.99	3.485 (4)	118
C2—H2*A*···N5^{vii}	0.97	2.55	3.487 (6)	162
C2—H2*B*···Cl2^{viii}	0.97	2.79	3.741 (6)	166
C5—H5···Cl2^{ix}	0.93	2.98	3.742 (5)	140
C5—H5···Cl2^{x}	0.93	2.90	3.344 (5)	111
C7—H7···Cl1^{xi}	0.93	2.94	3.438 (5)	115
C7—H7···O4^{i}	0.93	2.42	3.277 (6)	154

Symmetry codes: (i) $x, y+1, z$; (ii) $-x+1, -y+1, -z$; (iii) $x-1, y, z$; (iv) $-x+1, -y+1, -z+1$; (v) $-x+2, -y+1, -z$; (vi) $x+1, y, z$; (vii) $x, y-1, z$; (viii) $-x+2, -y+1, -z+1$; (ix) $-x+1, -y, -z+1$; (x) $x-1, y-1, z$; (xi) $x+1, y+1, z$.

4. Hirshfeld surface analysis

Hirshfeld surface (Spackman & Jayatilaka, 2009) and two-dimensional fingerprint plot analyses (Spackman & McKinnon, 2002) were performed using the program *CrystalExplorer* (Spackman *et al.*, 2021) to investigate and quantify the intermolecular interactions responsible for the consolidation of the crystal packing. For the sake of clarity, only interactions of the complex anion were considered.

As expected, the Hirshfeld surface (HS) of $[Mn(H_2O)_2Cl_2(C_3O_4H_2)]$ displays several prominent dark-red spots indicative of significant intermolecular interactions. A pair of red regions on opposite sides of the surface correspond to

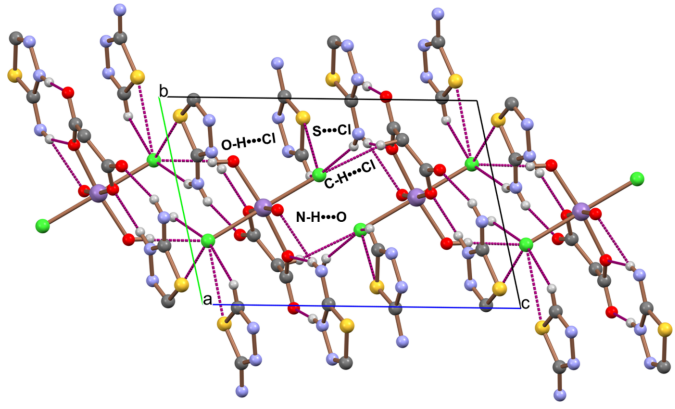

Figure 2
A view of the crystal packing of molecules along the *a* axis in the crystal structure of $(LH)_2[Mn(H_2O)_2Cl_2(C_3O_4H_2)]$ including the most important hydrogen-bonding interactions as colored dashed lines.

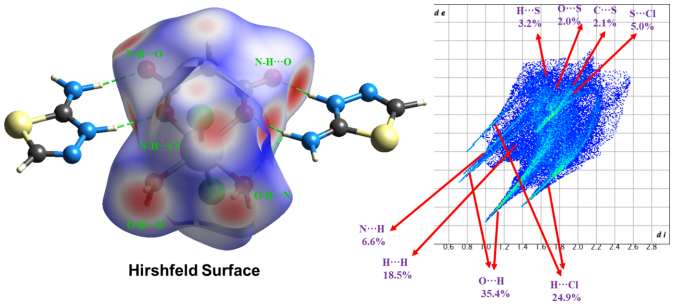

Figure 3
(Left) Hirshfeld surface of the $[Mn(H_2O)_2Cl_2(C_3O_4H_2)]^{2-}$ anion within the crystal structure of $(LH)_2[Mn(H_2O)_2Cl_2(C_3O_4H_2)]$; (right) two-dimensional fingerprint plot showing the contributions of different intermolecular contacts to the overall Hirshfeld surface area.

close N—H···O hydrogen-bonding interactions. Additionally, two red spots on the front side of the HS indicate short O—H···O and O—H···N contacts. A distinct red spot near the chloride atom suggests the presence of an N—H···Cl interaction (Fig. 3, left). The major intermolecular interactions contributing to the Hirshfeld surface area (97.7%) are visualized through the two-dimensional fingerprint plots (Fig. 3, right). These include O···H (35.4%), H···Cl (24.9%), H···H (18.5%), N···H (6.6%), S···Cl (5.0%), H···S (3.2%), C···S (2.1%), and O···S (2.0%) contacts. Minor interactions C···O (0.8%), C···H (0.6%), C···C (0.3%), and N···O (0.5%) collectively contribute less than 3% to the total HS area of $[Mn(H_2O)_2Cl_2(C_3O_4H_2)]$.

5. Database survey

A database survey conducted using the ConQuest program within the Cambridge Structural Database (CSD, Version 6.00, March 2025; Groom *et al.*, 2016) identified eight crystal structures containing metals such as cobalt, copper, and zinc, in which the ligand (*L*) coordinates monodentately to the metal cations *via* the endocyclic nitrogen atom at the 3-position (CSD refcode FICCOJ, Ishankhodzhaeva *et al.*, 1998; GAGVIV, GAGVOB, Wang *et al.*, 2010; GOKXOT, Khusenov *et al.*, 1998; NIYDII, Khusenov *et al.*, 1997; ZEKWOE, Gurbanov *et al.*, 2018; FUXKIW; Nuralieva *et al.*, 2025; JOJLUT, Kadirova *et al.*, 2022). Additionally, two structures were found where *L* acts as a bridging bidentate ligand, coordinating through two endocyclic nitrogen atoms to copper and silver cations (LIXSEQ, LIXSAM, Maekawa *et al.*, 1999). Furthermore, two complexes involving bismuth and antimony were reported where the nitrogen atom at the 3-position is protonated, resulting in non-coordinating thiadiazolium cations (GIKBIL, Antolini *et al.*, 1988; LEYHEC, Cornia *et al.*, 1994). Notably, no crystal structures have been reported so far in which a complex manganate anion is charge-balanced by a thiadiazolium cation.

6. Synthesis and crystallization

A solution of malonic acid (0.0052 g, 0.05 mmol) in 3 ml of ethanol was neutralized with sodium hydroxide (0.0052 g, 0.13 mmol) in 3 ml of ethanol and the mixture was heated at 323 K for 1 h under stirring. Separately, $MnCl_2{\cdot}4H_2O$ (0.099 g, 0.5 mmol) was dissolved in 3 ml of water, and 2-amino-1,3,4-thiadiazole (*L*) (0.101 g, 1 mmol) was dissolved in 3 ml of ethanol. The ligand solution was added dropwise to the $MnCl_2{\cdot}4H_2O$ solution under stirring, followed by the addition of the sodium malonate solution. Single crystals of the title complex, suitable for X-ray diffraction analysis, were obtained by slow evaporation of the solvent over 5 d. Yield: 78%, m.p. 493 K.

Table 2
Experimental details.

Crystal data	
Chemical formula	$(C_2H_4N_3S)_2[MnCl_2(C_3H_2O_4)(H_2O)_2]$
M_r	468.20
Crystal system, space group	Triclinic, $P\overline{1}$
Temperature (K)	293
a, b, c (Å)	8.4382 (3), 8.6103 (3), 12.6557 (4)
α, β, γ (°)	98.510 (2), 101.845 (3), 106.552 (3)
V (Å^3)	841.49 (5)
Z	2
Radiation type	Cu $K\alpha$
μ (mm^{-1})	12.01
Crystal size (mm)	0.16 × 0.14 × 0.09
Data collection	
Diffractometer	XtaLAB Synergy, Single source at home/near, HyPix3000
Absorption correction	Multi-scan (*CrysAlis PRO*; Rigaku OD, 2023)
T_{min}, T_{max}	0.282, 1.000
No. of measured, independent and observed [$I > 2\sigma(I)$] reflections	7249, 3240, 2690
R_{int}	0.071
$(\sin\theta/\lambda)_{max}$ (Å^{-1})	0.615
Refinement	
$R[F^2 > 2\sigma(F^2)]$, $wR(F^2)$, S	0.069, 0.192, 1.02
No. of reflections	3240
No. of parameters	226
No. of restraints	4
H-atom treatment	H atoms treated by a mixture of independent and constrained refinement
$\Delta\rho_{max}$, $\Delta\rho_{min}$ (e Å^{-3})	1.33, −1.16

Computer programs: *CrysAlis PRO* (Rigaku OD, 2023), *SHELXT* (Sheldrick, 2015*a*), *SHELXL* (Sheldrick, 2015*b*) and *OLEX2* (Dolomanov *et al.*, 2009).

7. Refinement

Crystal data, data collection and structure refinement details are summarized in Table 2. All hydrogen atoms were located from difference-Fourier maps and refined with a riding model; DFIX restraints were applied to some of the O—H bond lengths.

Acknowledgements

BT would like to acknowledge the FAIRE programme provided by the Cambridge Crystallographic Data Centre (CCDC) for the use of the Cambridge Structural Database (CSD) and associated software.

References

Ahmad, S., Alam, M. Z., Salma, U., Mohasin, M., Rahaman, P. F., Parveen, H. & Khan, S. A. (2024). *J. Mol. Struct.* **1312**, 138438.

Antolini, L., Benedetti, A., Fabretti, A. C. & Giusti, A. (1988). *J. Chem. Soc. Dalton Trans.* pp. 2501–2503.

Atashov, A., Azamova, M., Ziyatov, D., Uzakbergenova, Z., Torambetov, B., Holczbauer, T., Ashurov, J. & Kadirova, S. (2024). *Acta Cryst.* E**80**, 408–412.

Bondi, A. (1964). *J. Phys. Chem.* **68**, 441–451.

Chou, J. Y., Lai, S. Y., Pan, S. L., Jow, G. M., Chern, J. W. & Guh, J. H. (2003). *Biochem. Pharmacol.* **66**, 115–124.

Cornia, A., Fabretti, A. C., Grandi, R. & Malavasi, W. (1994). *J. Chem. Crystallogr.* **24**, 277–280.

Dolomanov, O. V., Bourhis, L. J., Gildea, R. J., Howard, J. A. K. & Puschmann, H. (2009). *J. Appl. Cryst.* **42**, 339–341.

Dolomanov, O. V., Bourhis, L. J., Gildea, R. J., Howard, J. A. K. & Puschmann, H. (2009). *J. Appl. Cryst.* **42**, 339–341.

Femi, A. J. & Ayoola, O. J. (2012). *J. Chem.* **9**, 2245–2254.

Groom, C. R., Bruno, I. J., Lightfoot, M. P. & Ward, S. C. (2016). *Acta Cryst.* B**72**, 171–179.

Gurbanov, A. V., Mahmoudi, G., Guedes da Silva, M. F. C., Zubkov, F. I., Mahmudov, K. T. & Pombeiro, A. J. (2018). *Inorg. Chim. Acta* **471**, 130–136.

Hu, Y., Li, C. Y., Wang, X. M., Yang, Y. H. & Zhu, H. L. (2014). *Chem. Rev.* **114**, 5572–5610.

Ishankhodzhaeva, M. M., Khusenov, K. S., Umarov, B. B., Parpiev, N. A. & Aleksandrov, G. G. (1998). *Russ. J. Inorg. Chem.* **43**, 1709–1711.

Kadirova, S., Torambetov, B., Razzokova, S., Uzakbergenova, Z., Abdreymov, A., Raxmonova, D. & Parpiev, N. (2022). *AIP Conf. Proc.* **2471**, 050034.

Khusenov, K., Umarov, B. B., Ishankhodzhaeva, M. M., Parpiev, N. A., Talipov, S. A. & Ibragimov, B. T. (1998). *Russ. J. Inorg. Chem.* **43**, 1841–1846.

Khusenov, K. S., Umarov, B. B., Ishankhodzhaeva, M. M., Parpiev, N. A., Talipov, S. A. & Ibragimov, B. T. (1997). *Russ. J. Coord. Chem.* **23**(8), 555–559.

Kinshakova, E., Torambetov, B., Bharty, M. K., Atashov, A., Rasulov, A., Kadirova, S. & Gonnade, R. G. (2025). *Acta Cryst.* E**81**, 569–572.

Kozieł, S., Wojtala, D., Szmitka, M., Sawka, J. & Komarnicka, U. K. (2024). *Front. Chem. Biol.* **3**, 1337372.

Lynch, D. E. (2002). *Acta Cryst.* E**58**, m577–m579.

Maekawa, M., Munakata, M., Kuroda-Sowa, T., Suenaga, Y. & Sugimoto, K. (1999). *Inorg. Chim. Acta* **290**, 153–158.

Nuralieva, G., Alieva, M., Torambetov, B., Christopher Leslee, D. B., Senthilkumar, B., Kaur, S., Dabke, N. D., Vanka, K., Ashurov, J., Kadirova, Sh. & Gonnade, R. (2025). *J. Mol. Struct.* **1338**, 142274.

Parmar, K. C. & Umrigar, N. H. (2017). *J. Chem. Pharm. Res.* **9**, 202–14.

Rigaku OD (2023). *CrysAlis PRO*. Rigaku Oxford Diffraction, Yarnton, England.

Sheldrick, G. M. (2015*a*). *Acta Cryst.* A**71**, 3–8.

Sheldrick, G. M. (2015*b*). *Acta Cryst.* C**71**, 3–8.

Spackman, M. A. & Jayatilaka, D. (2009). *CrystEngComm* **11**, 19–32.

Spackman, M. A. & McKinnon, J. J. (2002). *CrystEngComm* **4**, 378–392.

Spackman, P. R., Turner, M. J., McKinnon, J. J., Wolff, S. K., Grimwood, D. J., Jayatilaka, D. & Spackman, M. A. (2021). *J. Appl. Cryst.* **54**, 1006–1011.

Wang, N., Lin, Q. Y., Feng, J., Zhao, Y. L., Wang, Y. J. & Li, S. K. (2010). *Inorg. Chim. Acta* **363**, 3399–3406.

Zhu, H. L., Liu, Y. W., Tang, Z. M., Yin, F. J., Liu, W. W., Cao, Z. L., Bao, J., Li, M., Qin, L. Y. & Shi, D. H. (2017). *Inorg. Nano-Met. Chem.* **47**, 78–81.

supporting information

Acta Cryst. (2026). E**82**, 282-285 [https://doi.org/10.1107/S205698902600112X]

Synthesis, crystal structure and Hirshfeld surface analysis of bis(2-amino-1,3,4-thiadiazol-3-ium) diaquadichlorido(propanedioato-κ^2O^1,O^3)manganate(II)

Guzal Nuralieva, Mushtari Alieva, Ekaterina Kinshakova, Aziz Atashov, Jamshid Ashurov, Shakhnoza Kadirova and Batirbay Torambetov

Computing details

(I)

Crystal data

$(C_2H_4N_3S)_2[MnCl_2(C_3H_2O_4)(H_2O)_2]$
M_r = 468.20
Triclinic, $P\overline{1}$
a = 8.4382 (3) Å
b = 8.6103 (3) Å
c = 12.6557 (4) Å
α = 98.510 (2)°
β = 101.845 (3)°
γ = 106.552 (3)°
V = 841.49 (5) Å^3
Z = 2
$F(000)$ = 474
D_x = 1.848 Mg m^{-3}
Cu $K\alpha$ radiation, λ = 1.54184 Å
Cell parameters from 4604 reflections
θ = 3.7–71.7°
μ = 12.01 mm^{-1}
T = 293 K
Block, colourless
0.16 × 0.14 × 0.09 mm

Data collection

XtaLAB Synergy, Single source at home/near, HyPix3000 diffractometer
Detector resolution: 10.0000 pixels mm^{-1}
ω scans
Absorption correction: multi-scan (CrysAlis PRO; Rigaku OD, 2023)
T_{min} = 0.282, T_{max} = 1.000
7249 measured reflections
3240 independent reflections
2690 reflections with $I > 2\sigma(I)$
R_{int} = 0.071
θ_{max} = 71.5°, θ_{min} = 3.7°
h = −9→10
k = −10→10
l = −15→15

Refinement

Refinement on F^2
Least-squares matrix: full
$R[F^2 > 2\sigma(F^2)]$ = 0.069
$wR(F^2)$ = 0.192
S = 1.02
3240 reflections
226 parameters
4 restraints
Hydrogen site location: mixed
H atoms treated by a mixture of independent and constrained refinement
$w = 1/[\sigma^2(F_o^2) + (0.1342P)^2]$ where $P = (F_o^2 + 2F_c^2)/3$
$(\Delta/\sigma)_{max} < 0.001$
$\Delta\rho_{max}$ = 1.33 e Å^{-3}
$\Delta\rho_{min}$ = −1.15 e Å^{-3}

Special details

Geometry. All esds (except the esd in the dihedral angle between two l.s. planes) are estimated using the full covariance matrix. The cell esds are taken into account individually in the estimation of esds in distances, angles and torsion angles; correlations between esds in cell parameters are only used when they are defined by crystal symmetry. An approximate (isotropic) treatment of cell esds is used for estimating esds involving l.s. planes.

Fractional atomic coordinates and isotropic or equivalent isotropic displacement parameters (Å²)

	x	*y*	*z*	U_{iso}*/U_{eq}
Mn1	0.66473 (8)	0.47031 (8)	0.25494 (6)	0.0279 (3)
Cl1	0.46492 (14)	0.30744 (13)	0.05857 (10)	0.0351 (3)
Cl2	0.80574 (14)	0.63155 (15)	0.45305 (10)	0.0411 (3)
S1	0.14252 (15)	−0.09459 (14)	0.43995 (11)	0.0375 (3)
S2	1.29985 (14)	0.90727 (13)	0.05433 (10)	0.0341 (3)
O1	0.6478 (4)	0.2375 (4)	0.2996 (3)	0.0365 (8)
O3	0.8909 (4)	0.4502 (4)	0.2069 (3)	0.0323 (7)
O6	0.4238 (4)	0.4601 (4)	0.2983 (3)	0.0359 (8)
H6A	0.341222	0.420929	0.240211	0.054*
H6B	0.424141	0.558262	0.320859	0.054*
O4	1.0798 (4)	0.3374 (4)	0.1635 (3)	0.0364 (8)
O2	0.6671 (4)	−0.0131 (4)	0.2839 (3)	0.0377 (8)
O5	0.7029 (5)	0.6919 (4)	0.1910 (3)	0.0384 (8)
N4	1.0705 (5)	0.7358 (5)	0.1291 (3)	0.0320 (8)
H4	1.007128	0.654413	0.149434	0.038*
N1	0.3951 (5)	−0.0948 (5)	0.3625 (4)	0.0353 (9)
H1	0.482529	−0.062812	0.336449	0.042*
N2	0.3283 (5)	−0.2566 (5)	0.3715 (4)	0.0404 (10)
N6	1.2331 (5)	0.5837 (5)	0.0649 (4)	0.0394 (10)
H6C	1.176063	0.496823	0.083398	0.047*
H6D	1.314917	0.580369	0.034650	0.047*
N3	0.3647 (5)	0.1676 (5)	0.3959 (4)	0.0450 (11)
H3A	0.452465	0.211237	0.372695	0.054*
H3B	0.308031	0.228033	0.419026	0.054*
N5	1.0480 (5)	0.8885 (5)	0.1429 (4)	0.0403 (10)
C1	0.7247 (5)	0.1384 (5)	0.2811 (4)	0.0247 (8)
C3	0.9570 (5)	0.3379 (5)	0.2064 (4)	0.0229 (8)
C4	0.3170 (6)	0.0078 (6)	0.3961 (4)	0.0315 (10)
C6	1.1961 (5)	0.7190 (5)	0.0824 (4)	0.0295 (9)
C2	0.9015 (6)	0.1940 (6)	0.2619 (5)	0.0356 (11)
H2A	0.915146	0.098177	0.218655	0.043*
H2B	0.983146	0.221204	0.333611	0.043*
C7	1.1577 (6)	0.9867 (6)	0.1076 (4)	0.0381 (11)
H7	1.161906	1.096334	0.109999	0.046*
C5	0.1976 (6)	−0.2732 (6)	0.4114 (5)	0.0397 (11)
H5	0.136561	−0.373942	0.424126	0.048*
H5A	0.710 (7)	0.787 (3)	0.226 (4)	0.041 (15)*
H5B	0.653 (8)	0.687 (9)	0.124 (2)	0.07 (2)*

Atomic displacement parameters (Å²)

	U^{11}	U^{22}	U^{33}	U^{12}	U^{13}	U^{23}
Mn1	0.0236 (4)	0.0234 (4)	0.0443 (5)	0.0095 (3)	0.0184 (3)	0.0132 (3)
Cl1	0.0338 (6)	0.0290 (5)	0.0421 (7)	0.0051 (4)	0.0149 (5)	0.0099 (4)
Cl2	0.0329 (6)	0.0433 (6)	0.0445 (7)	0.0068 (5)	0.0157 (5)	0.0054 (5)
S1	0.0318 (6)	0.0388 (6)	0.0507 (8)	0.0115 (5)	0.0252 (5)	0.0168 (5)
S2	0.0293 (6)	0.0267 (5)	0.0494 (7)	0.0046 (4)	0.0185 (5)	0.0152 (5)
O1	0.0334 (17)	0.0294 (15)	0.062 (2)	0.0152 (13)	0.0291 (16)	0.0220 (15)
O3	0.0268 (15)	0.0286 (15)	0.051 (2)	0.0116 (12)	0.0214 (14)	0.0152 (14)
O6	0.0265 (16)	0.0317 (16)	0.052 (2)	0.0099 (13)	0.0160 (15)	0.0075 (14)
O4	0.0287 (16)	0.0332 (16)	0.058 (2)	0.0128 (13)	0.0246 (16)	0.0179 (15)
O2	0.0364 (18)	0.0256 (15)	0.061 (2)	0.0115 (13)	0.0274 (16)	0.0164 (14)
O5	0.050 (2)	0.0210 (15)	0.047 (2)	0.0128 (14)	0.0154 (18)	0.0101 (14)
N4	0.0280 (19)	0.0298 (18)	0.041 (2)	0.0056 (15)	0.0176 (17)	0.0121 (16)
N1	0.0266 (19)	0.034 (2)	0.048 (2)	0.0059 (16)	0.0197 (17)	0.0133 (17)
N2	0.033 (2)	0.0317 (19)	0.060 (3)	0.0081 (16)	0.020 (2)	0.0143 (19)
N6	0.038 (2)	0.0294 (19)	0.062 (3)	0.0119 (16)	0.028 (2)	0.0205 (19)
N3	0.039 (2)	0.036 (2)	0.071 (3)	0.0122 (18)	0.030 (2)	0.023 (2)
N5	0.038 (2)	0.031 (2)	0.059 (3)	0.0123 (17)	0.024 (2)	0.0124 (19)
C1	0.0233 (19)	0.0191 (18)	0.032 (2)	0.0033 (15)	0.0109 (17)	0.0068 (15)
C3	0.0144 (17)	0.0203 (17)	0.033 (2)	0.0007 (14)	0.0106 (16)	0.0062 (15)
C4	0.024 (2)	0.036 (2)	0.037 (3)	0.0092 (18)	0.0121 (18)	0.0112 (19)
C6	0.024 (2)	0.031 (2)	0.031 (2)	0.0023 (17)	0.0103 (18)	0.0081 (17)
C2	0.029 (2)	0.037 (2)	0.057 (3)	0.0173 (19)	0.025 (2)	0.024 (2)
C7	0.034 (2)	0.035 (2)	0.051 (3)	0.012 (2)	0.019 (2)	0.013 (2)
C5	0.036 (3)	0.032 (2)	0.054 (3)	0.007 (2)	0.019 (2)	0.014 (2)

Geometric parameters (Å, º)

Mn1—Cl1	2.6243 (13)	N4—N5	1.372 (5)
Mn1—Cl2	2.5363 (14)	N4—C6	1.347 (6)
Mn1—O1	2.136 (3)	N1—H1	0.8600
Mn1—O3	2.162 (3)	N1—N2	1.378 (5)
Mn1—O6	2.194 (3)	N1—C4	1.316 (6)
Mn1—O5	2.148 (3)	N2—C5	1.285 (7)
S1—C4	1.730 (4)	N6—H6C	0.8600
S1—C5	1.739 (5)	N6—H6D	0.8600
S2—C6	1.735 (4)	N6—C6	1.289 (6)
S2—C7	1.739 (5)	N3—H3A	0.8600
O1—C1	1.234 (5)	N3—H3B	0.8600
O3—C3	1.246 (5)	N3—C4	1.319 (6)
O6—H6A	0.8501	N5—C7	1.268 (6)
O6—H6B	0.8502	C1—C2	1.513 (6)
O4—C3	1.265 (5)	C3—C2	1.520 (6)
O2—C1	1.264 (5)	C2—H2A	0.9700
O5—H5A	0.850 (10)	C2—H2B	0.9700
O5—H5B	0.851 (10)	C7—H7	0.9300

N4—H4	0.8600	C5—H5	0.9300
Cl2—Mn1—Cl1	169.11 (5)	H6C—N6—H6D	120.0
O1—Mn1—Cl1	88.68 (11)	C6—N6—H6C	120.0
O1—Mn1—Cl2	92.49 (11)	C6—N6—H6D	120.0
O1—Mn1—O3	84.92 (12)	H3A—N3—H3B	120.0
O1—Mn1—O6	89.57 (12)	C4—N3—H3A	120.0
O1—Mn1—O5	170.65 (14)	C4—N3—H3B	120.0
O3—Mn1—Cl1	92.14 (10)	C7—N5—N4	109.2 (4)
O3—Mn1—Cl2	98.75 (10)	O1—C1—O2	122.8 (4)
O3—Mn1—O6	173.54 (11)	O1—C1—C2	121.6 (3)
O6—Mn1—Cl1	84.35 (10)	O2—C1—C2	115.4 (4)
O6—Mn1—Cl2	84.83 (10)	O3—C3—O4	123.0 (4)
O5—Mn1—Cl1	87.40 (11)	O3—C3—C2	122.4 (4)
O5—Mn1—Cl2	92.96 (11)	O4—C3—C2	114.5 (3)
O5—Mn1—O3	86.75 (13)	N1—C4—S1	111.1 (3)
O5—Mn1—O6	98.48 (14)	N1—C4—N3	124.6 (4)
C4—S1—C5	87.3 (2)	N3—C4—S1	124.3 (4)
C6—S2—C7	87.5 (2)	N4—C6—S2	109.2 (3)
C1—O1—Mn1	131.3 (3)	N6—C6—S2	126.6 (4)
C3—O3—Mn1	131.2 (3)	N6—C6—N4	124.2 (4)
Mn1—O6—H6A	109.4	C1—C2—C3	121.6 (4)
Mn1—O6—H6B	109.4	C1—C2—H2A	106.9
H6A—O6—H6B	104.5	C1—C2—H2B	106.9
Mn1—O5—H5A	125 (4)	C3—C2—H2A	106.9
Mn1—O5—H5B	120 (5)	C3—C2—H2B	106.9
H5A—O5—H5B	105 (6)	H2A—C2—H2B	106.7
N5—N4—H4	121.4	S2—C7—H7	121.5
C6—N4—H4	121.4	N5—C7—S2	117.0 (4)
C6—N4—N5	117.1 (4)	N5—C7—H7	121.5
N2—N1—H1	122.0	S1—C5—H5	122.2
C4—N1—H1	122.0	N2—C5—S1	115.5 (4)
C4—N1—N2	115.9 (4)	N2—C5—H5	122.2
C5—N2—N1	110.1 (4)		
Mn1—O1—C1—O2	−158.3 (4)	N2—N1—C4—N3	178.5 (5)
Mn1—O1—C1—C2	26.3 (7)	N5—N4—C6—S2	1.1 (5)
Mn1—O3—C3—O4	171.6 (3)	N5—N4—C6—N6	179.5 (5)
Mn1—O3—C3—C2	−11.2 (7)	C4—S1—C5—N2	−1.4 (5)
O1—C1—C2—C3	−32.3 (7)	C4—N1—N2—C5	0.7 (7)
O3—C3—C2—C1	24.6 (7)	C6—S2—C7—N5	0.6 (5)
O4—C3—C2—C1	−158.0 (4)	C6—N4—N5—C7	−0.6 (6)
O2—C1—C2—C3	152.0 (5)	C7—S2—C6—N4	−0.9 (4)
N4—N5—C7—S2	−0.2 (6)	C7—S2—C6—N6	−179.3 (5)
N1—N2—C5—S1	0.7 (6)	C5—S1—C4—N1	1.7 (4)
N2—N1—C4—S1	−1.8 (6)	C5—S1—C4—N3	−178.6 (5)

Hydrogen-bond geometry (Å, º)

D—H···*A*	*D*—H	H···*A*	*D*···*A*	*D*—H···*A*
O5—H5*A*···O2^{i}	0.85 (1)	1.93 (2)	2.761 (5)	166 (5)
O5—H5*B*···Cl1^{ii}	0.85 (1)	2.34 (1)	3.186 (4)	175 (7)
O6—H6*A*···O4^{iii}	0.85	2.08	2.853 (5)	151
O6—H6*B*···N2^{i}	0.85	2.06	2.866 (5)	158
N1—H1···O2	0.86	1.78	2.641 (5)	175
N3—H3*A*···O1	0.86	2.02	2.854 (5)	162
N3—H3*B*···Cl2^{iv}	0.86	2.39	3.207 (5)	158
N4—H4···O3	0.86	2.07	2.919 (5)	171
N6—H6*C*···O4	0.86	1.92	2.760 (5)	165
N6—H6*D*···Cl1^{v}	0.86	2.45	3.243 (4)	154
N6—H6*D*···Cl1^{vi}	0.86	2.99	3.485 (4)	118
C2—H2*A*···N5^{vii}	0.97	2.55	3.487 (6)	162
C2—H2*B*···Cl2^{viii}	0.97	2.79	3.741 (6)	166
C5—H5···Cl2^{ix}	0.93	2.98	3.742 (5)	140
C5—H5···Cl2^{x}	0.93	2.90	3.344 (5)	111
C7—H7···Cl1^{xi}	0.93	2.94	3.438 (5)	115
C7—H7···O4^{i}	0.93	2.42	3.277 (6)	154

Symmetry codes: (i) *x*, *y*+1, *z*; (ii) −*x*+1, −*y*+1, −*z*; (iii) *x*−1, *y*, *z*; (iv) −*x*+1, −*y*+1, −*z*+1; (v) −*x*+2, −*y*+1, −*z*; (vi) *x*+1, *y*, *z*; (vii) *x*, *y*−1, *z*; (viii) −*x*+2, −*y*+1, −*z*+1; (ix) −*x*+1, −*y*, −*z*+1; (x) *x*−1, *y*−1, *z*; (xi) *x*+1, *y*+1, *z*.